

Gap-soliton trapping in random one-dimensional gratings

Eduard N. Tsoy

Centre for Ultrahigh-Bandwidth Devices for Optical Systems, School of Physics, University of Sydney, Sydney, NSW 2006, Australia
and Physical-Technical Institute of the Uzbek Academy of Sciences, Mavlyanov Street 2-B, Tashkent-84, Uzbekistan

C. Martijn de Sterke

Centre for Ultrahigh-Bandwidth Devices for Optical Systems, School of Physics, University of Sydney, Sydney, NSW 2006, Australia

Fatkhulla Kh. Abdullaev

Physical-Technical Institute of the Uzbek Academy of Sciences, Mavlyanov Street 2-B, Tashkent-84, Uzbekistan
and Centre for Ultrahigh-Bandwidth Devices for Optical Systems, School of Physics, University of Sydney, Sydney, NSW 2006, Australia
(Received 4 July 2008)

The dynamics of gap solitons in random gratings is studied. We show that the influence of disorder is averaged over the soliton width, so that the soliton acts as a low-pass filter. The averaging results in an effective potential, which can trap solitons. The statistical properties of the potential are found. We show that soliton trapping is related to level crossing by a random function, which allows us to find the mean number of soliton reflections and the mean distance between consecutive reflections.

DOI: XXXX

PACS number(s): 42.25.Dd, 42.65.Tg, 42.70.Qs

Linear waves in random media experience Anderson localization [1], which means that the intensity of a wave decreases exponentially with propagation distance. On the other hand, it is known that nonlinear systems support the propagation of stable pulses, solitons, which are quite robust to external perturbations. The study of the interplay between the nonlinearity and disorder is a problem of great current interest [2–5].

Here we investigate the dynamics of gap solitons in one-dimensional (1D) gratings, in which the periodic variation of the refractive index is affected by fluctuations. Our motivation comes partly from recent gap-soliton experiments in the slow-light regime [6], where it was noted that the solitons travel not as slowly as expected from numerical simulations. A possible explanation was the influence of the randomness in the grating. Though our study does not confirm this, it reveals many interesting features of the slow-light regime in disordered gratings.

Our investigation also pertains to the analysis of the effect of disorder on the dynamics of localized waves in waveguide arrays. Recent studies of 1D [7,8] and 2D [9,10] arrays and lattices reveal ballistic transport, diffusive propagation, and localization, depending on the level of disorder. Another area of application of our results is the dynamics of gap solitons in Bose-Einstein condensates in optical lattices [11]. The manifestation of Anderson localization of matter waves in optical lattices was observed experimentally by several groups [12–14].

We demonstrate that gap solitons average the fluctuations of the random grating—i.e., that the fluctuations are integrated over the soliton's width. We provide clear evidence that the soliton acts as a *low-pass filter*, which reduces the high-wave-number components of the disorder. We also show that the filtered disorder creates an *effective potential*, so that the soliton can be trapped between the maxima of this potential. This approach allows us to find analytical expressions for the statistical properties of the soliton dynamics.

The propagation of light in 1D periodic media (Bragg

gratings) is described by the nonlinear coupled-mode equations [15]

$$\frac{i}{V_g} \frac{\partial E_{\pm}}{\partial t} \pm i \frac{\partial E_{\pm}}{\partial z} + \kappa(z) E_{\mp} + \Gamma(|E_{\pm}|^2 + 2|E_{\mp}|^2) E_{\pm} = 0, \quad (1)$$

where $E_{\pm}(z, t)$ are the forward- and backward-propagating field envelopes, respectively, V_g is the group velocity in the absence of the grating, $\kappa(z)$ is the coupling coefficient, Γ is the nonlinear coefficient, z is the spatial coordinate, and t is time. We consider amplitude modulations, taking $\kappa(z) = \kappa_0 + \kappa_1(z)$, where κ_0 is the mean value (MV) of the coupling coefficient and $\kappa_1(z)$ is Gaussian white noise with the correlation function $R_{\kappa}(z_1, z_2) = b^2 \delta(z_2 - z_1)$. For the parameters here, fluctuations in the grating's phase give similar results.

In the linear regime [$\Gamma = 0$ in Eq. (1)] and in the absence of disorder, the dispersion relation has a band gap: propagation of linear waves with frequencies ω inside the gap $|\omega| < \kappa_0 V_g$ is prohibited. However, a high-intensity wave induces nonlinear effects, which enable the existence of localized waves, or gap solitons [16] (see also Ref. [15] and references therein), with $|\omega| < \kappa_0 V_g$:

$$E_{\pm}(z, t) = A_{\pm} \operatorname{sech}[y \mp i\delta_s/2] e^{i(\theta_s + \mu)}, \quad (2)$$

where $A_{\pm} = \pm \sqrt{\kappa_0/\Gamma} [(1 \pm v)/(3 - v^2)]^{1/2} (1 - v^2)^{1/4} \sin \delta_s$, $y = \gamma \kappa_0 \sin \delta_s (z - v V_g t)$, $\theta_s = \gamma \kappa_0 \cos \delta_s (vz - V_g t)$, $\gamma = 1/\sqrt{1 - v^2}$, and $\exp(i\mu) = [-(e^{2y} + e^{-i\delta_s}) / (e^{2y} + e^{i\delta_s})]^{2v/(3 - v^2)}$. The parameter δ_s ($0 < \delta_s < \pi$) characterizes the soliton frequency inside the band gap. The values $\delta_s = 0$, $\pi/2$, and π correspond to the upper, middle, and lower edges of the band gap, respectively; $v V_g$ is the soliton velocity.

Numerical simulation of Eq. (1) shows two basic types of dynamics, depending on the disorder realization. In the first, the soliton propagates with fluctuating parameters in *one* direction, while the mean velocity slowly decreases due to radiation of linear waves. In the other type of the dynamics, the

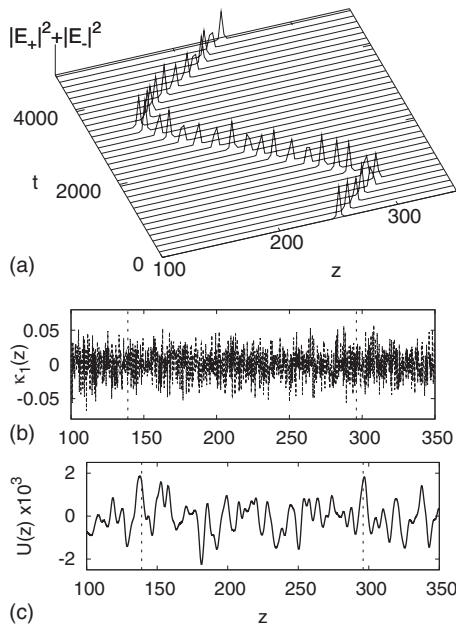


FIG. 1. (a) Soliton trapping in a particular realization of the disorder in numerical simulation of Eq. (1), with $v_0=0.1$, $\delta_s=0.5$, $b^2=10^{-5}$, and $\kappa_0=\Gamma=V_g=1$. (b) $\kappa_1(z)$ and (c) $U(z)$. Vertical dotted lines in (b) and (c) indicate the reflection points.

transform and k is the wave number. Therefore, we arrive at the important conclusion that $\tilde{\phi}(k)$ plays the role of a filter that modifies the disorder spectrum. Using the gap soliton solution (2), we find

$$\phi(z) = A \frac{\sinh(2\eta z)[2 + \cos \delta_s [\cosh(2\eta z) - \cos \delta_s]]}{(\cosh(2\eta z) + \cos \delta_s)^3}, \quad (5)$$

where $A \equiv 8V_g \kappa_0^2 \sin^3 \delta_s / [(3-v^2)\gamma\Gamma]$ and $\eta \equiv \gamma \kappa_0 \sin \delta_s$. Generally, $\phi(z)$ depends on v ; however, for $v^2 \ll 1$, the correction is negligible, $\sim v^2$. Since soliton trapping is realized when $v^2 \ll 1$, we ignore the dependence of $\phi(z)$ on v , taking $v=0$ in Eq. (5).

For low velocities, $P \approx mV$, where $m=4\kappa_0(7 \sin \delta_s - 4\delta_s \cos \delta_s)/(9\Gamma V_g)$ is the soliton ‘‘mass’’ [17] and $V=vV_g=d\xi/dt$ is its velocity. Then (3) is the equation of motion of a classical particle subjected to the force f , or moving in the potential $U(\xi)=U(\xi_0)-\int_{\xi_0}^{\xi} f(x)dx$, where $U(\xi_0)$ is such that the MV of $U(\xi)$ is zero. The effective potential obtained using $\phi(z)$ from Eq. (5) for the realization of $\kappa_1(z)$ in Fig. 1(b) is shown in Fig. 1(c). The potential peaks close to the reflection points, indicating that it gives a good description of the soliton dynamics.

Equation (3) conserves the soliton’s ‘‘mechanical’’ energy $E=mV^2/2+U(\xi)=E_0$, where E_0 is the initial energy. This guarantees that in the adiabatic limit, the soliton is always trapped by the effective potential, since U can have, in principle, peaks with values larger than E_0 . However, the lower the disorder level, the longer the grating length for which the soliton is definitely reflected back or trapped. To study this quantitatively we need the statistical properties of the potential.

Applying Eq. (5), we obtain the statistical properties of the force acting on the soliton and of the corresponding potential. Since the convolution is a linear function, the correlation function (CF) of the force is expressed via the autocorrelation of $\phi(z)$ (see [18], Sec. 10):

$$R_f(\xi_2 - \xi_1) = b^2 \int_{-\infty}^{\infty} \phi(z) \phi(\xi_2 - \xi_1 + z) dz. \quad (6)$$

For $\delta_s \ll 1$, R_f reduces to

$$R_f(\xi_2 - \xi_1) \approx \frac{A^2 b^2 [1 + (1 - \zeta \coth \zeta)(1 + 3 \operatorname{cosech}^2 \zeta)]}{\eta \sinh^2 \zeta}, \quad (7)$$

where $\zeta \equiv \eta(\xi_2 - \xi_1)$. Since the CF of the force depends on $(\xi_2 - \xi_1)$, the force is a stationary random process on ξ with a Gaussian distribution and zero mean value.

The standard deviation $\sigma_f = R_f^{1/2}(0)$ of the force can be found explicitly from Eqs. (5) and (7), but has a cumbersome form. However, using approximation (7), we easily find

$$\sigma_f^2 \approx \frac{A^2 b^2}{15\eta} = \frac{64}{135} \frac{V_g^2 \kappa_0^3 \delta_s^5}{\Gamma^2} b^2. \quad (8)$$

Thus, given a grating, the ratio σ_f/b depends only on the detuning δ_s when $v^2 \ll 1$. The thick (thin) dashed curve in Fig. 2 is the exact result from (6) [an approximation based on Eq. (8)].

soliton is trapped between two points in the grating; see Fig. 1(a). A naive explanation of the trapping is that the soliton is reflected between two spikes of the random modulation $\kappa_1(z)$. However, a comparison of the soliton trajectory [see Fig. 1(a)] and the corresponding realization of $\kappa_1(z)$ [see Fig. 1(b)] shows that (i) the reflection points do not necessarily coincide with peaks of $\kappa_1(z)$ and (ii) that there are high-level spikes of $\kappa_1(z)$ between the reflection points. In fact, the soliton is trapped between two maxima of an effective potential. In Fig. 1, as well as in the other numerical examples, we take $\kappa_0=\Gamma=V_g=1$.

When the disorder is weak and the soliton velocity is small ($v^2 \ll 1$), the dynamics is adiabatic. This means that the soliton retains its shape and radiates some energy. Therefore, one can use the effective particle approximation [17] to describe the soliton dynamics. Then, the variation of the field momentum $P = -i \int_{-\infty}^{\infty} (E_+^* \partial_z E_+ + E_-^* \partial_z E_-) dz$ is described by

$$\frac{dP}{dt} = -V_g \int_{-\infty}^{\infty} 2\kappa_1(z) \frac{\partial}{\partial z} \operatorname{Re}[E_+^*(z,t)E_-(z,t)] dz \equiv f, \quad (3)$$

where $\operatorname{Re}[\cdot]$ denotes the real part. The product $E_+^*(z,t)E_-(z,t)$ is a function of $z-\xi(t)$, where ξ is the soliton center, so we can write

$$f(\xi) = \int_{-\infty}^{\infty} \kappa_1(z) \phi(\xi - z) dz,$$

$$\phi(\xi - z) = -2V_g \frac{\partial}{\partial z} \operatorname{Re}[E_+^*(z,t)E_-(z,t)]. \quad (4)$$

Since the force f is a convolution of ϕ and the noise $\kappa_1(z)$, then $\tilde{f}(k) = \tilde{\phi}(k)\tilde{\kappa}_1(k)$, where the tilde means the Fourier

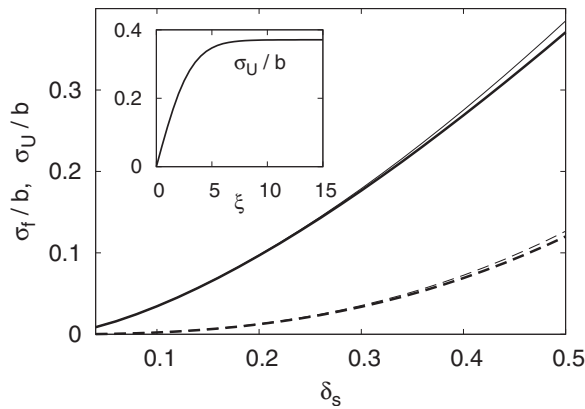


FIG. 2. Parameters σ_f (dashed curve) and $\sigma_U(8/\eta)$ (solid curve) versus δ_s . The thick curves correspond to exact results, found from Eqs. (6) and (9), respectively. The thin curves are approximations, found from Eqs. (8) and (10), respectively. The inset shows $\sigma_U(\xi)$ at $\delta_s=0.5$.

162 The potential U , as an integral of the force, can be con-
 163 sidered as a Wiener-Levy-type process. A standard Wiener-
 164 Levy process is an integral of white noise [18], while $f(z)$ is
 165 colored noise with the CF given by Eq. (6). The CF
 166 $R_U(\xi_1, \xi_2)$ and standard deviation $\sigma_U(\xi)=R_U^{1/2}(\xi, \xi)$ of U can
 167 be written as (see [18], Sec. 10)

$$168 \quad R_U(\xi_1, \xi_2) = h(\xi_2 - \xi_0) - h(\xi_2 - \xi_1) + h(\xi_1 - \xi_0),$$

$$169 \quad \sigma_U^2(\xi) = 2h(\xi - \xi_0), \quad h(\xi) = \int_0^\xi (\xi - x)R_f(x)dx. \quad (9)$$

170 Therefore, the potential U is a nonstationary random process
 171 with a Gaussian distribution and zero mean value. In the
 172 limit $\delta_s \ll 1$, the function $h(z)$ is written as

$$173 \quad h(\xi) \approx \frac{A^2 b^2}{4\eta^3} \left[\frac{1}{3} + \frac{1 - \eta\xi \coth(\eta\xi)}{\sinh^2(\eta\xi)} \right] \rightarrow \frac{16 V_g^2 \kappa_0 \delta_s^3 b^2}{27 \Gamma^2},$$

$$174 \quad \xi \rightarrow \infty. \quad (10)$$

176 Both σ_f and $\sigma_U(\infty)$ increase with the grating strength κ_0 and
 177 are inversely proportional to Γ .

178 The inset in Fig. 2 shows σ_U versus ξ . Since, for large ξ ,
 179 σ_U tends to a constant, the nonstationarity of $U(\xi)$ is pro-
 180 nounced only for $\xi \lesssim 1/\eta$. The asymptotic value of σ_U at
 181 large ξ can be used as an upper estimate of the standard
 182 deviation of U . The thick and thin solid lines in the main part
 183 of Fig. 2 correspond to the exact σ_U and its approximation,
 184 found from Eq. (10), at $\xi=8/\eta$, respectively. The depen-
 185 dences in Fig. 2 represent the transformation coefficient from
 186 the level of the disorder in κ to that in f or U for $\kappa_0=\Gamma$
 187 $=V_g=1$. These dependences can be rescaled for the other
 188 parameter values by using (8) or (10). Also, since the prob-
 189 ability for $U(\xi)$ to have a maximum larger than $3\sigma_U$ is very
 190 low, the condition $mV_0^2/2=3\sigma_U$, where $V_0=v_0V_g$, defines a
 191 threshold velocity above which the soliton propagates with-
 192 out reflections.

193 We now consider the trapping of the soliton between
 194 peaks of the potential U . Suppose that the soliton is reflected

at position ξ_r . This means that $U(\xi)$ reaches the level E_0 at
 $\xi=\xi_r$. Therefore, we arrive at the well-known problem of a
 level crossing by a random function [18,19]. The complete
 solution, which includes the derivation of the probability
 density, of this problem for $U(\xi)$ is complicated, because
 $U(\xi)$ is a nonstationary random process. Here we consider
 only the MV of the number of reflection points (NRPs) and
 of the length of intervals between reflections (IBRs). We fol-
 low the standard derivation [19] which we now briefly
 outline.

For an arbitrary random function $u(z)$, the mean value L_B
 of the sum of all intervals, where $u(z)$ is below the level a , in
 the interval $z=[z_0, z_0+L]$ is $L_B=L\int_{-\infty}^a P_u du$, where P_u is the
 probability density of u . The number of crossings of level a
 by $u(z)$, where only crossing points with $u'(z)\equiv du/dz>0$
 are counted, is [19] $n_B=\int_{z_0}^{z_0+L} u'(z)\theta[u'(z)]\delta[u(z)-a]dz$,
 where $\theta(x)$ is the Heaviside step function. The value of n_B
 equals the number of the IBRs and is approximately half of
 the total NRPs. Then the MV of n_B is written as [19]

$$\langle n_B \rangle = \int_{z_0}^{z_0+L} dz \int_0^\infty u' P_2(u, u') du', \quad (11)$$

where $P_2(u, u')$ is the joint probability distribution of u and
 u' . The mean length l_B of a single IBR can be estimated as

$$l_B = L_B / \langle n_B \rangle. \quad (12)$$

We apply these results for $u \equiv U(\xi)$ and $a=E_0$. We use the
 fact that $U(\xi)$ is a normal process and that U and U' are
 jointly normal. Then we get

$$L_B = L\Phi(E_0/\sigma_U), \quad \langle n_B \rangle = \int_{\xi_0}^{\xi_0+L} J(E_0, z) dz, \quad (13)$$

where

$$\Phi(z) = \frac{1}{\sqrt{2\pi}} \int_{-\infty}^z \exp(-x^2/2) dx, \quad (223)$$

$$J(a, z) = \frac{\sigma_f \sqrt{1-\rho^2}}{2\pi\sigma_U} e^{-a^2/(2\sigma_U^2)} [e^{-\tau^2/2} + \sqrt{2\pi}\tau\Phi(\tau)], \quad (224)$$

$$\rho(z) = \frac{1}{\sigma_f \sigma_U} \int_0^z R_f(z) dz, \quad \tau = \frac{\rho}{\sqrt{1-\rho^2}} \frac{a}{\sigma_U}. \quad (14) \quad (225)$$

To obtain numerical estimates of the MVs, we take
 $U(\xi_0)=0$, so that $E_0=mV_0^2/2$. The disorder is modeled by
 using a random number generator with the standard devia-
 tion $\sigma_{RNG}=0.02$. Then, for the spatial step $h=0.025$, we get
 $b^2=h\sigma_{RNG}^2=10^{-5}$. The dependence of l_B and $\langle n_B \rangle$ on L for
 $\delta_s=0.5$ and $v_0=0.1$ found from Eqs. (12)–(14) is shown in
 Fig. 3. For a propagation length $L=100$, the MV of the IBR
 is $l_B \approx 4 \times 10^3 \gg L$. At this length, $\langle n_B \rangle=0.05$ and grows lin-
 early with L . Thus, in gratings with 2% disorder and L
 $=1000$, solitons are reflected in about half the realizations. In
 numerical simulations of Eq. (1), though $U(\xi_0)$ does not nec-
 essarily equal zero, we have qualitative agreement with the
 dependences in Fig. 3.

The function $J(E_0, z)$ is the density of the number of in-

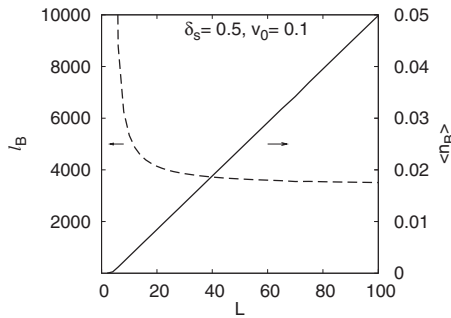


FIG. 3. Mean length l_B of the IBRs (dashed line) and the mean value $\langle n_B \rangle$ of the NRPs with positive derivative (solid line) versus L , for $b^2=10^{-5}$, $\delta_s=0.5$, and $v_0=0.1$.

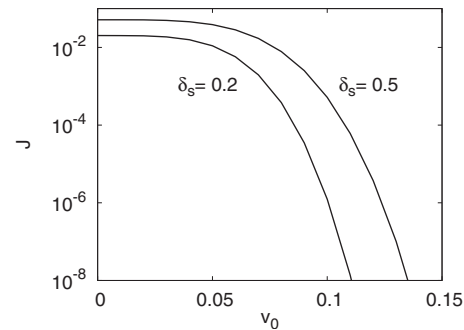


FIG. 4. Density $J(E_0, 8/\eta)$ versus v_0 for $\delta_s=0.2$ and 0.5 and $b^2=10^{-5}$. We take $U(\xi_0)=0$.

240 intersections of $U(\xi)$, where $U'(\xi) > 0$ at the intersections, with
 241 level E_0 . The value $J(E_0, z)$ tends to a constant as $z \rightarrow \infty$:
 242 $J(E_0, \infty) = \sigma_f \exp\{-E_0^2/[2\sigma_U^2(\infty)]\}/[2\pi\sigma_U(\infty)]$. Then $J(E_0, \infty)$
 243 is an essential parameter that characterizes the number of
 244 reflections, $\langle n_B \rangle \approx LJ(E_0, \infty)$, which is related also to the rela-
 245 tive number of realizations where the reflection can occur.
 246 Taking $\langle n_B \rangle = 1$, we obtain the characteristic propagation
 247 length $L_{SR} = 1/J(E_0, \infty)$, on which a single reflection of the
 248 soliton is almost certain. The density $J(E_0, \infty)$ depends expo-
 249 nentially on the initial velocity and detuning; for example, in
 250 the case $U(\xi_0)=0$, $J(E_0, \infty) \sim \exp[-3\kappa_0 v_0^4/(16\delta_s b^2)]$.

251 Figure 4 shows $J(E_0, 8/\eta)$, found from Eq. (14), versus
 252 the initial velocity parameter v_0 for different δ_s and $U(\xi_0)$
 253 $= 0$. The density J decreases rapidly for $v_0 \gtrsim 0.1$. However,
 254 for $v_0 \lesssim 0.1$, $L_{SR} \sim 10^2 - 10^4$. Since fiber gratings with $\kappa_0 L$
 255 $\sim 10^2 - 10^3$ are feasible, the results should be observable in
 256 experiments. In real systems the pulse is injected from one
 257 side of a grating. The trapping then manifests itself by a
 258 reflection of the soliton.

259 The soliton dynamics described here applies in the adia-

batic regime with weak disorder. Numerical simulations of 260
 Eq. (1) show that stronger disorder may result in soliton 261
 splitting, but this is beyond the scope of this work. 262

In conclusion, we explain the soliton trapping in random 263
 grating by using a concept of disorder filtering by the soliton. 264
 The influence of the disorder is averaged such that only the 265
 slowly varying components affect the propagation. The fil- 266
 tering results in an effective trapping potential. Since aver- 267
 aging is a linear transformation, the statistical properties of 268
 the potential can be found exactly. We demonstrate that the 269
 probability of soliton trapping is related to the probability of 270
 zero crossings by the potential and use this to find the mean 271
 values of NRPs and IBRs. Because of the filtering action, we 272
 expect the results for noise with a finite correlation length 273
 less than the soliton width to be similar to those obtained 274
 here with δ -correlated noise. 275

The authors thank Dr. A. Asatryan for useful discussions. 276
 F.Kh.A. acknowledges the University of Sydney for Support. 277 AQ:
 This work was supported by the Australian Research Council 278 #1
 under the ARC Centres of Excellence Program. 279

280
 281
 282

- 283 [1] P. W. Anderson, *Philos. Mag. B* **52**, 505 (1985).
 284 [2] S. A. Gredeskul and Y. S. Kivshar, *Phys. Rep.* **216**, 1 (1992).
 285 [3] R. Knapp, *Physica D* **85**, 496 (1995).
 286 [4] J. Garnier, *SIAM J. Appl. Math.* **58**, 1969 (1998).
 287 [5] F. Kh. Abdullaev and J. Garnier, *Prog. Opt.* **48**, 35 (2005).
 288 [6] J. T. Mok *et al.*, *Nat. Phys.* **2**, 775 (2006).
 289 [7] Y. V. Kartashov and V. A. Vysloukh, *Phys. Rev. E* **72**, 026606
 290 (2005).
 291 [8] Y. Lahini *et al.*, *Phys. Rev. Lett.* **100**, 013906 (2008).
 292 [9] T. Pertsch *et al.*, *Phys. Rev. Lett.* **93**, 053901 (2004).
 293 [10] T. Schwartz *et al.*, *Nature (London)* **446**, 52 (2007).
 294 [11] O. Morsch and M. Oberthaler, *Rev. Mod. Phys.* **78**, 179
 295 (2006).

- [12] T. Schulte *et al.*, *Phys. Rev. Lett.* **95**, 170411 (2005). 296
 [13] Y. P. Cheng *et al.*, e-print arXiv:cond-mat/0710.5187 (2007). 297
 [14] G. Roati *et al.*, e-print arXiv:cond-mat/0804.2609 (2008). 298
 [15] C. M. de Sterke and J. E. Sipe, *Prog. Opt.* **33**, 203 (1994). 299
 [16] A. B. Aceves and S. Wabnitz, *Phys. Lett. A* **141**, 37 (1989); D. 300
 N. Christodoulides and R. I. Joseph, *Phys. Rev. Lett.* **62**, 1746 301
 (1989). 302
 [17] N. G. R. Broderick and C. M. de Sterke, *Phys. Rev. E* **51**, 303
 4978 (1995); **58**, 7941 (1998). 304
 [18] A. Papoulis, *Probability, Random Variables and Stochastic 305*
Processes, 3rd ed. (McGraw-Hill, New York, 1991). 306
 [19] V. I. Tikhonov and V. I. Khimenko, *Spikes of Trajectories of 307*
Random Processes (Nauka, Moscow, 1987). 308

AUTHOR QUERIES —

#1 see H. 22 memo.